Heliyon 6 (2020) e04114

Contents lists available at ScienceDirect

Heliyon

journal homepage: www.cell.com/heliyon

Research article

Rapid and specific detection of oxidized LDL/β2GPI complexes via facile lateral flow immunoassay

Xian Wen Tan [a], Fumiaki Takenaka [b], Hironori Takekawa [c], Eiji Mastuura [a,b,c,d,*]

[a] Department of Cell Chemistry, Okayama University Graduate School of Medicine, Dentistry and Pharmaceutical Sciences, Okayama, Japan
[b] Collaborative Research Center (OMIC), Okayama University Graduate School of Medicine, Dentistry and Pharmaceutical Sciences, Okayama, Japan
[c] Faculty of Medicine, Okayama University, Okayama, Japan
[d] Neutron Therapy Research Center, Okayama University, Okayama, Japan

ARTICLE INFO

Keywords:
Biological sciences
Antibody
Biochemistry
Lipid peroxidation
Health sciences
Oxidized LDL (oxLDL)
β2-glycoprotein I (β2GPI)
OxLDL-β2GPI
Lateral flow immunoassay (LFIA)
Enzyme-linked immunosorbent assay (ELISA)
Point-of-care

ABSTRACT

β2-Glycoprotein I (β2GPI) forms indissociable complex with oxidized LDL (oxLDL) into proatherogenic oxLDL/β2GPI complex through a specific ligand known as 7-ketocholesteryl-9-carboxynonanoate (oxLig-1). Recent discoveries have demonstrated the atherogenicity of these complexes in patients of both systemic and non-systemic autoimmune diseases. Hence, serological level of oxLDL/β2GPI complexes may represent one crucial clinical parameter for disease prognosis of atherosclerosis-related diseases. Herein, we established a simple, specific and rapid gold nanoparticle (GNP) based lateral flow immunoassay (LFIA) to quantify oxLDL/β2GPI complexes from test samples. Specificities of hybridoma cell-derived monoclonal antibodies against antigen, optimal conditions for conjugation of antibody with GNP, and sensitivity of oxLDL/β2GPI LFIA in comparison to an ELISA-based detection method were assessed accordingly. The established oxLDL/β2GPI LFIA was capable of detecting oxLDL/β2GPI specifically without interference from autoantibodies and solitary components of oxLDL/β2GPI present in test samples. A significant correlation ($R^2 > 0.8$) was also obtained with the oxLDL/β2GPI LFIA when compared to the ELISA-based detection. On the whole, the oxLDL/β2GPI LFIA remains advantageous over the oxLDL/β2GPI ELISA. The unnecessary washing step, short developmental and analytical time support facile and rapid detection of oxLDL/β2GPI as opposed to the laborious ELISA system.

1. Introduction

The pathogenesis of lifestyle disease such as atherosclerosis is closely associated with metabolic abnormalities of lipoproteins [1]. Its onset and progression have been intimately linked to lipid peroxidation of low-density lipoprotein (LDL) within the arterial intima. Nearly 50% composition of LDL is mainly composed of cholesterol and cholesteryl esters (CEs), thus it is highly susceptible to oxidation by reactive oxygen species (ROS) such as superoxide anions ($O_2^{\cdot}$) and hydroxyl radicals (·OH) [2]. Oxidized LDL (OxLDL), the oxidized form of LDL, acts as a pro-inflammatory chemoattractant that activate atherothrombotic immune response by promoting pro-thrombotic endothelial dysfunction, synthesis and secretion of chemotactic cytokines. These abnormalities promote recruitments of macrophages and their subsequent activation and intracellular lipid accumulation within atherosclerotic lesions [3, 4].

The prevalence of serological antiphospholipid antibodies (aPL), such as anticardiolipin (aCL) antibodies and lupus anticoagulant (LA), is one of the clinical characteristics and prognoses of antiphospholipid syndrome (APS) [5, 6, 7, 8]. Monomeric β2-glycoprotein I (β2GPI) or phospholipid-bound β2GPI is perceived as the major immunogen held accountable for the induction of aPL in APS patients [9, 10, 11, 12]. β2GPI, a 50 kDa endogenous plasma protein [13], notoriously interact with anionic phospholipids such as phosphatidylserine (PS), cardiolipin (CL), and oxidized LDL (oxLDL) to form protein-lipid complexes [14, 15, 16, 17]. The phospholipid-binding site of β2GPI was previously identified in its domain V, at the sequence of K^{282}NKEKK^{287} [17]. β2GPI recognizes the structural part of 7-ketocholesteryl-9-carboxynonanoate (oxLig-1), a specific ligand in oxLDL, to form indissociable oxLDL/β2GPI complexes [18]. In the presence of IgG anti-oxLDL/β2GPI autoantibodies, the uptake of oxLDL/β2GPI complexes by macrophages through their Fcγ receptors was enhanced significantly and has notably accelerated the formation of foam cells and progression of atherosclerosis [18, 19, 20, 21, 22]. Aside from APS [23], our previous studies have also demonstrated the atherogenicity of these complexes in patients of non-systemic autoimmune

* Corresponding author.
E-mail address: eijimatu@md.okayama-u.ac.jp (E. Mastuura).

https://doi.org/10.1016/j.heliyon.2020.e04114
Received 7 April 2020; Received in revised form 15 May 2020; Accepted 28 May 2020

diseases, such as diabetes mellitus [24] and chronic renal diseases [25]. Intrinsically, serological level of oxLDL/β2GPI complexes may represent a crucial clinical parameter for disease prognosis and risk stratification of atherosclerosis-related diseases.

Presently, serological levels of oxLDL/B2GPI complexes are measurable by enzyme-linked immunosorbent assay (ELISA). We have formerly used a lupus associated APS in NZW x BXSB F1 (W/B F1) mouse model to establish a monoclonal IgG (known as 'WB-CAL-1') that develop specificity towards oxLDL/β2GPI complexes. WB-CAL-1 is highly specific towards the open form of β2GPI that has formed complex with oxLDL and not the closed form of β2GPI protein [14, 26, 27]. We later fabricated another monoclonal antibody, 3H3, which share similar antigen-specificity as WB-CAL-1, yet with improved affinity and specificity towards β2GPI complexed with oxLDL [28]. The established indirect sandwich (Figure 1) oxLDL/B2GPI ELISA utilizes two different antibodies to target on two different epitopes on oxLDL/β2GPI complex. The coated monoclonal 3H3 antibody on ELISA plate acts as the primary antibody that specifically recognizes β2GPI complexed with oxLDL only while the secondary antibody, 2E10 binds to apolipoprotein B100 (apoB100) on oxLDL of the complex [29].

Despite the applicability of our established oxLDL/β2GPI complexes ELISA, it incurs common drawbacks as with other conventional ELISA techniques. High labor-intensiveness, sophisticated operational steps, long incubation time, and cost-inefficiency are known drawbacks that limit the operational efficiency of diagnostic kits especially for high-throughput applications [30]. With the growing demand for rapid and cost-efficient point-of-care diagnostic means, novel technologies have been introduced to further improve current clinical diagnostics into favorable alternatives. Lateral flow immunoassays (LFIA) have gained interest in diagnostic applications due to their numerous advantages that complies with the World Health Organization (WHO) guidelines. Criteria such as being cost-efficient, offering high sensitivity and specificity, easy to use, expeditious, sturdy, and being practical are benchmarked as essential settings for diagnostic tests in developing countries [31]. Herein, we attempted to establish a simple LFIA system that can rapidly quantify oxLDL/β2GPI complexes within 20 min.

2. Methodology

2.1. Production and purification of anti-β2GPI (3H3) and anti-human apoB100 (2E10) antibodies

Anti-β2GPI (3H3) antibody- and anti-human apoB100 (2E10) antibody-producing hybridoma cells were cultivated respectively in Iscove's Modified Dulbecco's Medium (IMDM) with L-glutamine, phenol red, Hepes and sodium pyruvate (Fujifilm Wako Pure Chemical Corporation, Osaka, Japan), supplemented with 2.5 % (v/v) fetal bovine serum and 100 units of penicillin-streptomycin. Cells were cultivated at 37 °C, 5 % humidity for 4–5 days before culture supernatant was collected for antibody purification.

Cells suspension was gathered and centrifuged at 1,500 rpm, 4 °C for 5 min to collect culture supernatant. Respective antibodies were isolated from culture supernatants by purifications through rProteinA Sepharose Fast Flow (GE Healthcare Bio-sciences, Tokyo, Japan). Briefly, rProteinA Sepharose Fast Flow affinity medium was pre-equilibrated with 5 bed volumes of loading buffer (50 mM Tris/3.5 M NaCl/0.1 % NaN_3, pH8.8). Then respective culture supernatants were pre-mixed with loading buffer at 1:1 ratio, and subsequently loaded onto the column. Unbound contaminants were eliminated by washing the column with additional 5 bed volumes of loading buffer until the absorbance of collected effluent at 280 nm read less than 0.01 AU. Bound proteins were eluted by addition of elution buffer (0.17 M glycine-HCl, pH 2.3). The eluate was fractionated at 1mL and each fraction was subsequently neutralized by 3 mL neutralizing buffer (1 M Tris-HCl, pH 8.8). Elution was performed until the absorbance of collected eluate at 280 nm read less than 0.01 AU. Antibody-containing fractions were then combined and concentrated with Amicon® ultra 0.5 mL centrifugal filters (50K cut-off) (Merck Millipore, Darmstadt, Germany). Concentration of recovered antibody was determined via Pierce™ BCA Protein Assay Kit (ThermoFisher Scientific, Rockford, IL). Purity and antibody activity were verified via SDS-PAGE (10–20 % gels) and ELISA respectively.

2.2. Isolation of LDL from human serum

LDL was isolated from human serum pool (Cosmo Bio, Tokyo, Japan) through a single spin density gradient ultracentrifugation as per method of Swinkels, Hak-Lemmers and Demacker [32] with slight modifications. Briefly, 3 different density-adjusted solutions (DAS) (DAS 1: 1.006 g/cm^3; DAS 2: 1.019 g/cm^3; DAS 3: 1.063 g/cm^3), each containing 1 mM EDTA, were prepared by adjusting the solutions' densities with potassium bromide (KBr). Thawed human serum pool was pre-mixed with KBr at a volume-to-weight ratio of 13 mL serum to 1.82 g KBr. Mixture was left to homogenize via gentle low-speed stirring on ice bath for 10 min. Solutions were loaded slowly into polycarbonate (80PC bottle [C]) bottle (Hitachi-Koki, Tokyo, Japan) in the order of plasma (23.6 mL) > DAS 3 (18.2 mL) > DAS 2 (18.2 mL) > DAS 1 (10 mL). Sample-loaded bottles were then subjected to ultracentrifugation via RP45T rotor-equipped SCP85H ultracentrifuge machine (Hitachi-Koki, Tokyo, Japan) at 100, 000 x g, 4 °C for 24 h. After centrifugation, VLDL- and chylomicrons-containing fraction was carefully removed and

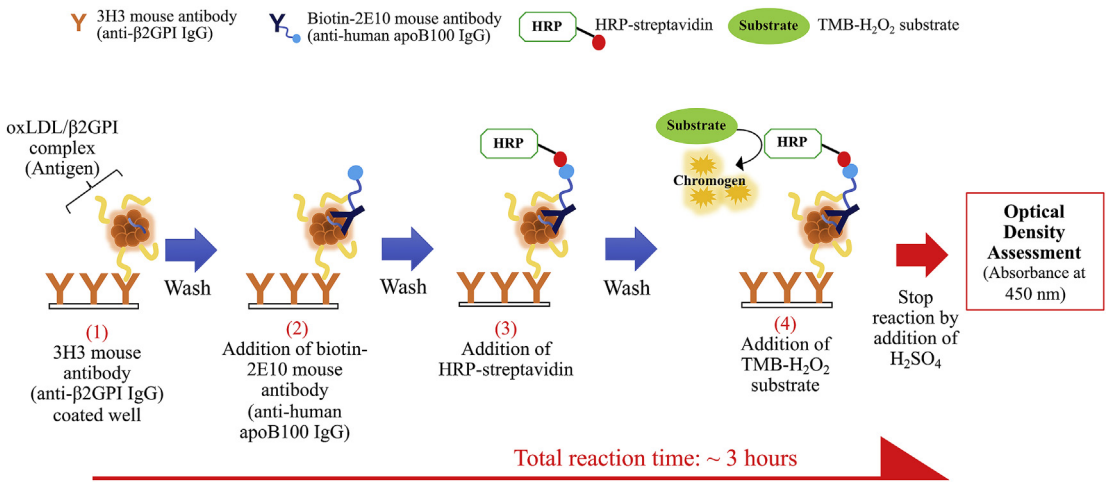

Figure 1. Schematic representation of oxLDL/β2GPI ELISA workflow and its principle.

subsequently followed by acquisition of LDL-containing fraction. LDL fraction was later concentrated via amicon ultra centrifugal filter unit (10K cut-off) (Merck Millipore, Darmstadt, Germany) and dialyzed against PBS buffer (pH 7.4) overnight in preparation for oxidation. Concentration of acquired LDL fraction of apolipoprotein B100 (apoB100) equivalent was determined through Pierce™ BCA Protein Assay Kit (ThermoFisher Scientific, Rockford, IL).

2.3. Preparation of chemically oxidized LDL (Cu^{2+}-oxLDL) and Cu^{2+}-oxLDL/β2GPI

Concentration of LDL was adjusted to 100 μg/mL apoB100 equivalent and subsequently chemically oxidized by 5 μM copper (II) sulphate ($CuSO_4$) at 37 °C for 16 h. Oxidation was terminated by addition of EDTA (final concentration of 1 mM) to the reaction mixture. For negative control, EDTA was added to the LDL and $CuSO_4$ mixture at 0 time (t = 0). Aliquots of the resulting reaction mixtures were taken for thiobarbituric reactive substance (TBARS) assay and agarose gel electrophoresis while the remaining was dialyzed against PBS buffer containing 1 mM EDTA overnight.

Complexation of Cu^{2+}-oxLDL and β2GPI was performed by mixing both component at a ratio of 2:1. Final concentration of Cu^{2+}-oxLDL and β2GPI were adjusted to 100 μg/mL and 50 μg/mL respectively. The reaction mixture was then incubated at 37 °C for 16 h and was terminated by freezing the samples at -80 °C. Complexation of Cu^{2+}-oxLDL and β2GPI was verified through agarose gel electrophoresis and ELISA assay.

2.4. Thiobarbituric reactive substance (TBARS) assay

Oxidation of LDL was evaluated via TBARS assay by measuring malondialdehyde (MDA), a byproduct of lipid peroxidation [33]. Briefly, reference standards comprised of different concentrations of MDA (0–60 nmoles), negative control and Cu^{2+}-oxLDL fraction were respectively mixed with reaction buffer (consisting of 1 part of 0.67 % (w/v) thiobarbituric acid and 1 part of 0.2 % (w/v) trichloroacetic acid. Mixtures were homogenized briefly and incubated at 100 °C water bath for 30 min. Reaction mixtures were cooled prior to fluorescence spectroscopy analysis at excitation and emission wavelengths of 515 nm and 553 nm respectively. TBARS values of samples were presented as nmol MDA equivalent per mg protein.

2.5. Agarose gel electrophoresis of LDL and related components

Agarose gel electrophoresis of plasma, LDL, Cu^{2+}-oxLDL, β2GPI, and Cu^{2+}-oxLDL/β2GPI was performed with TITAN Gel universal plate (Helena Laboratories, Beamount, TX). All components (except plasma; 2 μL loading volume) were loaded at a fixed protein equivalent content of 8 μg to the dedicated wells on agarose gel films. Then gel electrophoresis was conducted with barbital electrophoresis buffer (containing 10 mM barbital, 50 mM sodium diethylbarbiturate, 1 mM EDTA, and 15 mM NaN_3) at 90 V for 30 min. The gel films were then fixed in fixing solution [60 % (v/v) EtOH and 10 % (v/v) CH_3COOH in H_2O] for 15 min and then dried in drying oven at 60 °C for 20 min. The dried gel films were then stained for protein with Amido black 10B and stained for lipids with Fat Red 7B respectively.

2.6. Preparation of biotin-conjugated anti-β2GPI (3H3) and gold nanoparticle (GNP)-conjugated anti-apoB100 (2E10) antibodies

Biotinylation of 3H3 antibody was performed using commercially available Biotin Labelling Kit-NH_2 (Dojindo Laboratories, Kumamoto, Japan) as per product's instructions. Briefly, 200 μg of 3H3 antibody was added to the filtration tube (from kit) and final volume was topped up to 200 μL with WS Buffer (from kit). Mixture was then homogenized thoroughly through gentle pipetting and followed by centrifugation at 8,000 x g, 4 °C for 10 min. Next, NH_2 reactive biotin was reconstituted in 10 μL DMSO and the whole volume of reconstituted NH_2 reactive biotin was added to the filtration tube together with 100 μL Reaction Buffer (from kit). The reaction mixture was then mixed thoroughly by gentle pipetting, then incubated at 37 °C for 10 min. Thereafter, 100 μL of WS Buffer was then added to the filtration tube, and followed by centrifugation at 8,000 x g, 4 °C for 10 min. Content in filtration tube was then washed twice with 200 μL of WS Buffer and followed by centrifugation at 8,000 x g, 4 °C for 10 min, to remove excess unconjugated biotin molecules. The biotin-3H3 conjugate was later recovered in 200 μL PBS buffer. Concentration of biotinylated-3H3 was determined via Pierce™ BCA Protein Assay Kit (ThermoFisher Scientific, Rockford, IL).

Commercially available gold conjugation kit (Naked Gold Conjugation Kit (20 nm), Bioporto Diagnostics, Denmark) was used to conjugate 2E10 antibody with GNP. The spectral absorptivity and average particle size of GNP were characterized via UV-visible spectrophotometer (Bio-Spec-Nano, Shimadzu, Japan) and Malvern Zetasizer Nano ZSP (Malvern Instruments, Malvern, UK) respectively. 2E10 antibody was conjugated with 20 nm GNP as per protocol specified by the manufacturing company with slight modification. Briefly, 2E10 antibody which was originally suspended in PBS buffer were exchanged with ultrapure water (Direct-Q® Water Purification System, Merck Millipore, Germany) via Amicon® Ultra 0.5 mL Centrifugal Filters 10K (Merck Millipore, Germany). The 20 nm GNP (Naked Gold Conjugation Kit (20 nm), Bioporto Diagnostics, Denmark) has an original optical density (O.D) at 15 A.U. and was then adjusted to O.D 6 A.U and O.D 1.5 A.U. by diluting the GNP with ultrapure water (Direct-Q® Water Purification System, Merck Millipore, Germany) respectively. Diluted GNP of O.D 1.5 A.U. was used for optimization of GNP-antibody conjugation. Different concentrations of 2E10 antibody (0–25 μg/mL) and pH of coating buffer (pH 7.3-pH 9.6) were tested to identify the optimal concentration of antibody and pH for successful and stable conjugation of 2E10 antibody to GNP. Concentration of 2E10 antibody was adjusted with ultrapure water (Direct-Q® Water Purification System, Merck Millipore, Germany) while pH of coating buffer was adjusted with 0.2 M K_2CO_3. The stability of GNP-2E10 antibody was verified via visual examination of physical colour change, spectral absorption profile and salt aggregation assay [with 10 % (w/v) NaCl]. The identified and selected optimal antibody concentration was up-scaled 4x to accommodate the production of stable GNP-2E10 with diluted GNP of O.D 6 A.U. and pH of coating buffers was adjusted with 0.2 M K_2CO_3 accordingly. The 2E10 antibody, at a final concentration of 60 μg/mL was added to the pH- and O.D-adjusted GNP (pH 9.2) and set aside to incubate at room temperature for 1 h. The reaction was later terminated by addition of stabilizing buffer containing bovine serum albumin (BSA) at a ratio of 1:5 and left to incubate further at room temperature for 16 h.

2.7. Immunoassays

A total of 9 commercial human serum standards were provided by Corgenix Medical Corporation (Broomfield, CO). The standard serum samples were acquired from normal and APS/systemic lupus erythematosus (SLE) patients. These standard serum samples, alongside with the chemically synthesized Cu^{2+}-oxLDL/β2GPI complexes were used in the following immunoassays:

2.7.1. Anti-β2GPI-, anti-oxLDL- & anti-oxLDL/β2GPI IgG ELISA

ELISA for anti-β2GPI-, anti-oxLDL- & anti-oxLDL/β2GPI IgG were prepared by coating Cu^{2+}-oxLDL (50 μg/mL), β2GPI (50 μg/mL), and Cu^{2+}-oxLDL/β2GPI (50 μg/mL), in Hepes buffer (10 mM Hepes and 150 mM NaCl, pH 7.4), onto respective Nunc MaxiSorp™ flat-bottom microplates (ThermoFisher Scientific, Middletown, VA) and incubated at 4 °C overnight. Microplate was then blocked with 1 % (w/v) BSA at room temperature for 2 h. Human serum standards (50-fold dilution in Hepes buffer) were loaded to the wells at 100 μL per well and incubated at room temperature for 2 h. Wells were then incubated with HRP-conjugated anti-human IgG (Goat F(ab')2 Anti-Human IgG (Fab')2

(HRP)-ab98535, Abcam, Eugene, OR) in a dilution 1:5000, at room temperature for 1 h. Wells were washed extensively with 0.05 % (v/v) Tween-20 in 0.01 M PBS buffer at each interval. 3,3′,5,5′-tetramethylbenzidine (TMB)-H_2O_2 chromogenic substrate was added to wells (incubated for 30 min) for color development and reaction was later terminated with 0.3 N H_2SO_4 solution. O.D of samples was then measured at 450 nm and reference wavelength at 600 nm via microplate reader (Tecan Sunrise, Switzerland).

2.7.2. OxLDL/β2GPI ELISA

ELISA for oxLDL/β2GPI complexes was performed as per method of Ames, Ortiz-Cadenas, Torre, Nava, Oregon-Miranda, Batuca, Kojima, Lopez and Matsuura [29] with slight modifications (Figure 1). Briefly, 8 μg/mL of 3H3 antibody, in Hepes buffer (10 mM Hepes and 150 mM NaCl, pH 7.4), was coated (100 μL per well) onto Immulon 2HB microplate (ThermoFisher Scientific, Middletown, VA) at 4 °C overnight. Microplate was then blocked with 1 % (w/v) BSA at room temperature for 2 h. Reference blank (Hepes buffer), Cu^{2+}-oxLDL/β2GPI complexes as reference standards (0.01–2.00 μg/mL), and serum samples (100-fold dilution in Hepes buffer) were loaded to the wells at 100 μL per well and incubated at room temperature for 1 h. Wells were then incubated with biotinylated anti-apoB100 antibody (2E10) and subsequently followed by HRP-labelled streptavidin for 1 h respectively. Wells were washed extensively with 0.05 % (v/v) Tween-20 in 0.01 M PBS buffer at each interval. TMB-H_2O_2 chromogenic substrate was added to wells (incubated for 30 min) for color development and reaction was later terminated with 0.3 N H_2SO_4 solution. O.D of samples was then measured at 450 nm and reference wavelength at 600nm via microplate reader (Tecan Sunrise, Switzerland).

2.7.3. OxLDL/β2GPI LFIA

The workflow for oxLDL/β2GPI LFIA was depicted in Figure 2A. Briefly two components were prepared separately. Component A consisted of a mixture of 2.5 μL biotin-3H3 antibody (100 μg/mL) and serum samples (25 μL; 2x dilution with sample buffer – borate buffer supplemented with 0.5 % (w/v) BSA, pH 7.4) or Cu^{2+}-oxLDL/β2GPI reference standard (25 μL; concentrations in the range of 0.01–50.0 μg/mL) while component B consisted of 2.5 μL GNP-2E10 antibody (60 μg/mL) in 25 μL sample buffer. Both prepared mixtures were homogenized by gentle pipetting and incubated at room temperature for 15 min. Sample buffer, LDL (2 μg/mL), Cu^{2+}-oxLDL (2 μg/mL) and β2GPI (2 μg/mL) were used as negative controls to assess the possibilities of these components for non-specific binding. Then, sequential LFIA detection strip incubation began with 1-minute incubation in mixture of component A and later followed by 4 min incubation in mixture of component B. Images of developed LFIA detection strips were captured by camera (without

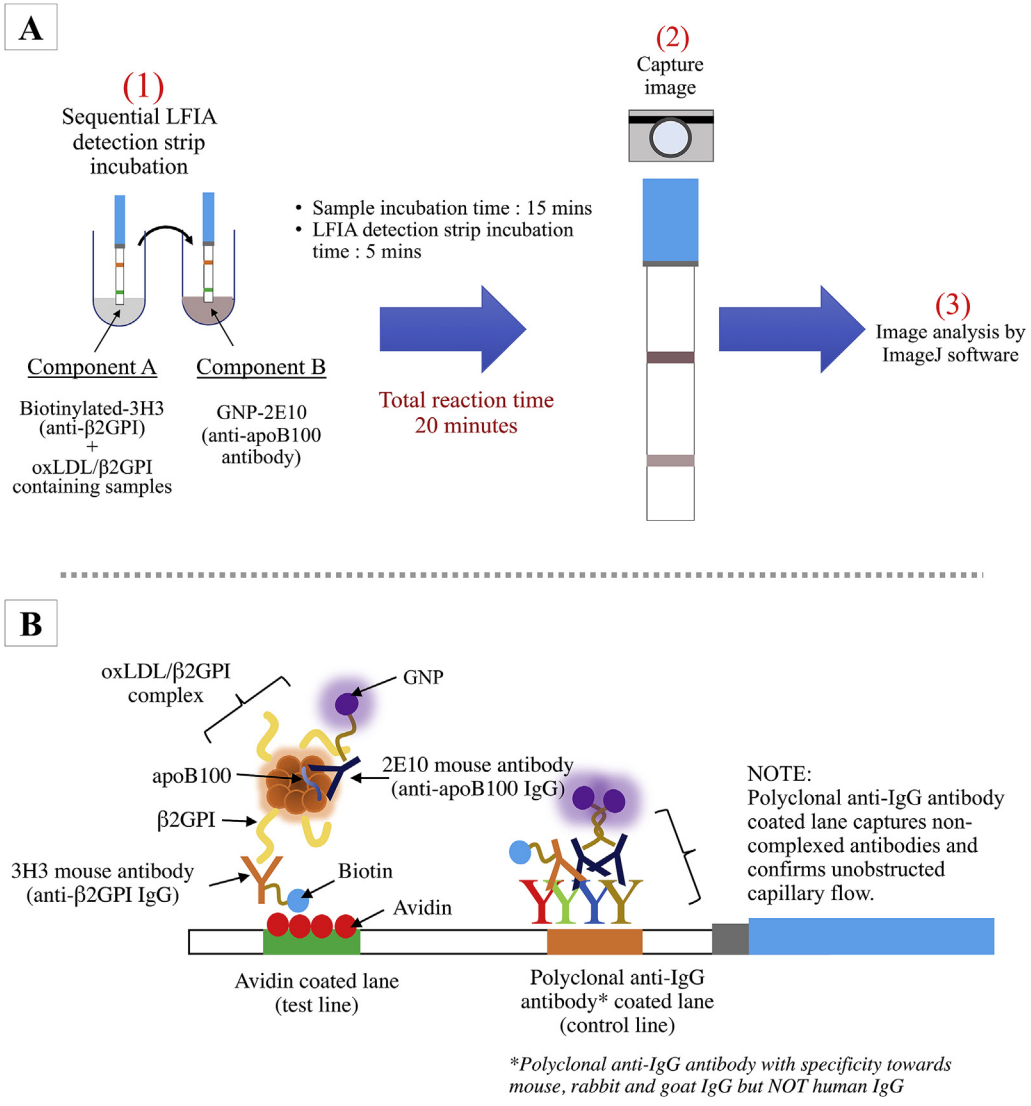

Figure 2. Graphical representations of (A) oxLDL/β2GPI LFIA workflow and (B) principle of assay.

flashlight). The intensities of the test and control lines were measurable via ImageJ software for data analysis.

2.7.4. Statistical analysis

The four parametric logistic (4PL) analytical tool from MyAssays Analysis Software Solutions (http://myassays.com) was used to generate four parametric logistic (4PL) standard curves and automated calculations of oxLDL/β2GPI contents in unknown samples of both ELISA- and LFIA-based analyses. Correlation of oxLDL/β2GPI contents in serum samples analyzed by both ELISA- and LFIA-based was determined by interpolating data derived from both analyses. A R^2 value >1.6 is considered as a significant correlation.

3. Results and discussions

3.1. Purification and validation of 3H3- and 2E10-antibodies

Hybridoma cells derived 3H3- and 2E10-monoclonal antibodies were purified through Protein A affinity chromatography. The purities and stabilities of 3H3- and 2E10-monoclonal antibodies were verified with SDS-PAGE (Figure 3). Under reducing condition, antibody fragments with band sizes at 50 kDa (heavy chains) and 25 kDa (light chains) were observed. Full size antibodies were still observable at 150 kDa while majority of the antibodies have been fragmented into their respective heavy chains (approximately 50 kDa) and light chains (approximately 25 kDa). Reactivities of 3H3 and 2E10 antibodies were further tested in ELISA and LFIA.

3.2. Cu^{2+}-oxLDL and Cu^{2+}-oxLDL/β2GPI

Lipid peroxidation rate of LDL was evaluated via thiobarbituric acid reactive substance (TBARS) assay (Figure 4A). The assay quantifies malondialdehyde (MDA), a fluorogenic byproduct resulting from the hydrolytic reaction of lipid hydroperoxides [33]. Through a quick comparison between negative control (oxidation reaction of LDL halted by the addition of EDTA at time '0') and oxLDL (oxidation at 37 °C for 16 h), a distinguishable difference in MDA content between two samples was observed. The negative control fraction recorded a MDA content of 13.4 nmol/mg protein while the oxLDL sample recorded a MDA content of 499.5 nmol/mg protein. The high content of MDA found in the Cu^{2+}-oxLDL denoted oxidation of LDL to Cu^{2+}-oxLDL.

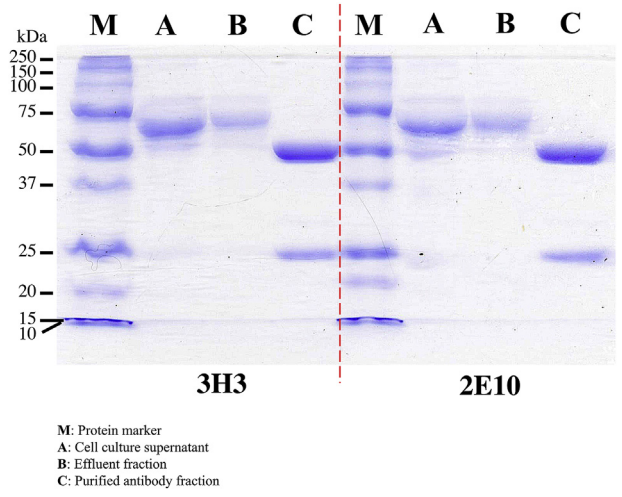

Figure 3. SDS-PAGE gel image of different fractions derived from Protein A antibody purification of 3H3- and 2E10-monoclonal antibodies. Samples were reduced with 2-mercaptoethanol at 99 °C for 5 min prior to SDS-PAGE. 'M' denotes protein marker; 'A' denotes cell culture supernatant; 'B' denotes effluent fraction; 'C' denotes purified antibody fraction.

The existence of Cu^{2+}-oxLDL and successful complexation of Cu^{2+}-oxLDL/β2GPI were further verified with agarose gel electrophoresis (Figure 4B). Migrations of Cu^{2+}-oxLDL, Cu^{2+}-oxLDL/β2GPI and their respective controls (LDL and β2GPI) were observed via Fat Red 7B and Amido Black 10B staining. Fat red 7B selectively stains the lipids while Amido Black 10B stains the protein. Due to the staining nature of staining dyes, migration profile of β2GPI in the agarose gel was only detectable in Amido Black stained gels. Among all loaded samples, the negatively charged oxLDL migrated furthest away from the origin of loading point and its negative charge acquired from $CuSO_4$-mediated oxidation were neutralized through its complexation with β2GPI. As such the migration profile of oxLDL/β2GPI fell in between those of β2GPI and Cu^{2+}-oxLDL.

3.3. Characterizations of GNP and GNP-2E10

Colloidal gold (such as GNP used in this study), carbon nanotubes, and fluorescent dyes (e.g. quantum dots) are some of the available labels applicable for antibody conjugation. The intense colour, homogeneity, high stability in both solution and solid forms, and nonessential visual-developmental process are among the advantageous points of colloidal GNP label as compared to the other two counterparts [30, 34]. Fluorescence-based labels such as carbon nanotubes and quantum dots often encounter drawbacks such as high background noise, photosensitivity, and require additional developmental process with specific visualizer to visualize [30].

The spectral absorptivity of GNP was confirmed through UV-visible spectrophotometer. It showed a characteristic wine-red colour with a maximum spectral absorptivity (λ max) at approximately 520 nm. The average hydrodynamic size of bare GNP as determined through dynamic light scattering (DLS) was measured at 35 nm (Figure 5A). After conjugation with 2E10 antibody, the average hydrodynamic size of GNP-2E10 increased to 43 nm.

Optimal antibody concentration and pH for stable GNP-2E10 conjugate were determined via UV-visible spectrometer and salt aggregation assay. Concentration of 2E10 antibody beyond 8 μg/mL instigated a slight red shift in λ max of GNP, and thus indicating successful conjugation of GNP and 2E10 antibody. The interaction between antibodies and the surface of GNP prompted a slight shift in surface plasmon resonance band of GNP (λ max at ~520 nm) and concurrently increased its average hydrodynamic size [35].

Through salt aggregation assay, unstable GNP-antibody conjugate with incomplete antibody coating will aggregate and resulted in visually assessible colour shift of conjugate solution, from its original red colour to purplish black [36, 37]. In this study, upon the addition of 10 % (w/v) NaCl, solutions of GNP-2E10 conjugates with concentration of 2E10 antibody below 8 μg/mL documented a colour change from red to purplish-black with visible black precipitate (Figure 5B). Due to incomplete coating of 2E10 onto the surface of GNP, the GNP aggregated and fell out of the solution while completely coated GNP-2E10 (with concentration of 2E10 beyond 8 μg/mL) did not aggregate in high-salt solution. Minimal concentration of 2E10 antibody required to produce stable conjugate was logged at 8 μg/mL. In order to produce stable GNP-2E10 conjugate, additional 20 % of minimum 2E10 antibody concentration (10 μg/mL) was recommended (as per manufacturer's recommendation) and hence was selected for up-scaled production of stable GNP-2E10.

As for the pH factor of GNP dispersion medium, GNP-2E10 conjugates were mostly stable in dispersion medium of pH 9.2 and above. Although the UV-visible spectral profile of GNP-2E10 in different pH dispersion medium showed a slight red shift in λmax of GNP, salt aggregation assay revealed GNP-2E10 dispersed in medium beyond pH 9.2 did not aggregate in high-salt solution (Figure 5C) hence suggesting the formation of stable GNP-2E10 conjugates. The pH of GNP dispersion medium has been shown to alter the surface chemistry and charge of antibodies and GNP, and immensely affects the stability and robustness of the resulting GNP-antibody conjugate [38]. For upscaled production of GNP-2E10, the

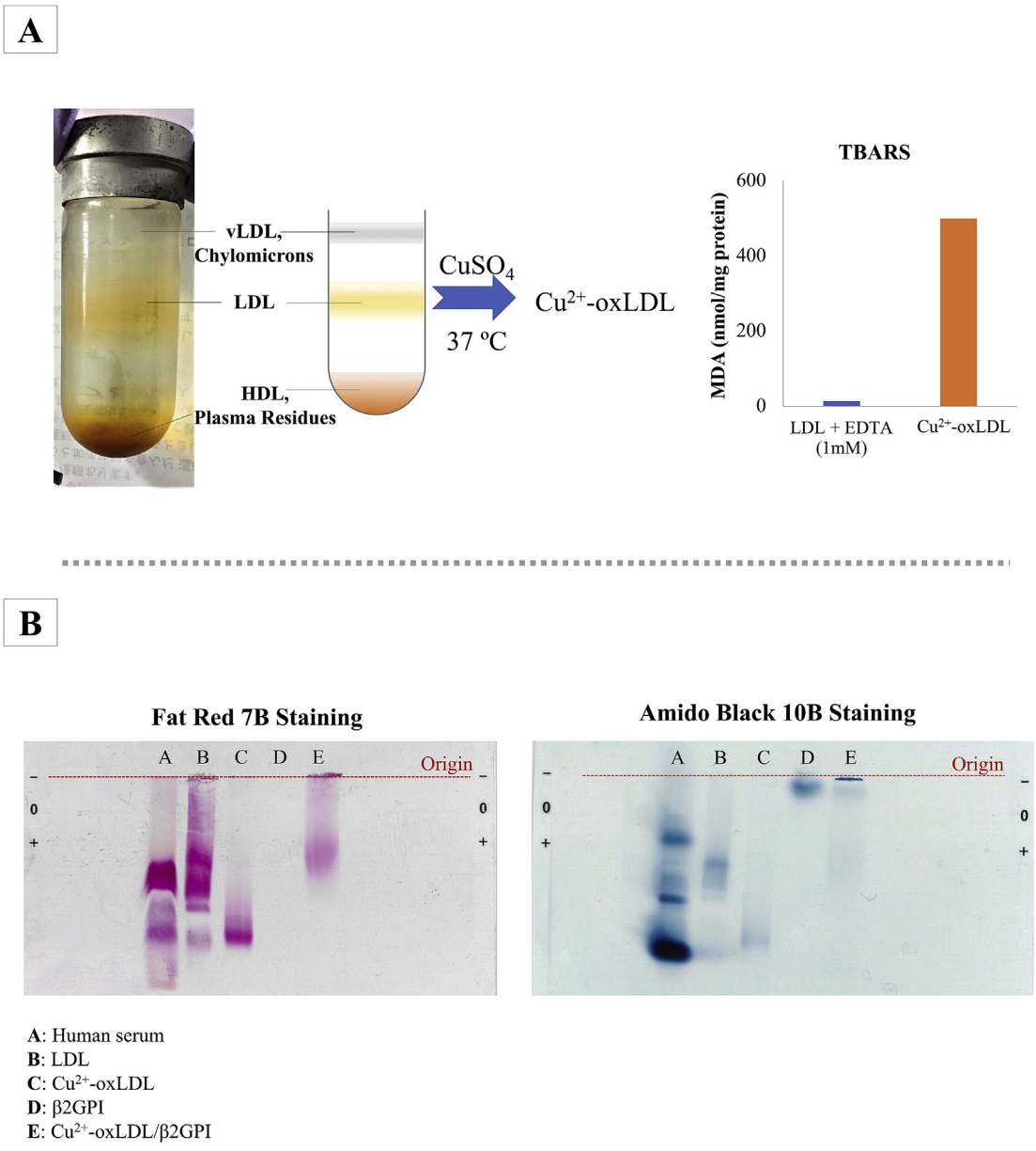

Figure 4. (A) LDL was extracted human serum pool through single spin density gradient ultracentrifugation and LDL-containing fraction was subsequently oxidized chemically with $CuSO_4$. TBARS assay was performed to evaluate the oxidation of LDL and TBARS values were expressed in nmol MDA per mg protein. (B) Electrophoretic migrations of human pool serum, LDL, Cu^{2+}-oxLDL, β2GPI, Cu^{2+}-oxLDL/β2GPI on agarose gel. Amido Black 10B dye was used to stain protein while Fat Red 7B dye was used to stain lipids.

selected optimal concentration of 2E10 antibody (10 μg/mL in GNP O.D 1.5 A.U.) was increased 4x to produce stable GNP-2E10 of O.D 6 A.U. With 60 μg/mL 2E10 antibody and a coating buffer of pH 9.2, the GNP-2E10 remained stable and did not aggregate in 10% (w/v) NaCl solution (Figure 5A).

3.4. Principles of oxLDL/β2GPI LFIA

The portability and user-friendliness of LFIA has revolutionized the point-of-care platform for rapid disease diagnosis and risk stratification [30]. Herein, we demonstrated the use of LFIA-based platform to assess serological level of oxLDL/β2GPI in a simple, rapid and specific manners. The principle of oxLDL/β2GPI LFIA (Figure 2B) is based upon the specific immunoreactions between the antigen (oxLDL/β2GPI) and two antibodies (3H3 and 2E10 antibodies) on a customized nitrocellulose membrane. The oxLDL/β2GPI LFIA in this study utilized two different mouse-derived monoclonal antibodies were advantageous owing to their respective specificities and consistent affinities towards specific epitopes on the antigen (oxLDL/β2GPI). 3H3 antibody only recognizes β2GPI portion of the antigenic oxLDL/β2GPI and not solitary β2GPI while 2E10 antibody binds to apoB100 of oxLDL. Although the two monoclonal antibodies used were affixed with different conjugators, their specificities and affinities towards their respective epitopes remained unhindered.

The LFIA test strips from Bioporto Diagnostics used in this study were composed of a nitrocellulose analytical membrane with wicking pad attached at one end to haul fluids up the membrane by capillarity. On the nitrocellulose membrane, two approximately 1 mm line are coated with avidin (test line) and a mixture of polyclonal anti-mouse/rabbit/goat IgG antibody (control line) respectively. The avidin coated test line captures biotinylated components while polyclonal anti-IgG antibody coated on the control line captures excess IgG/gold nanoparticle conjugated IgG.

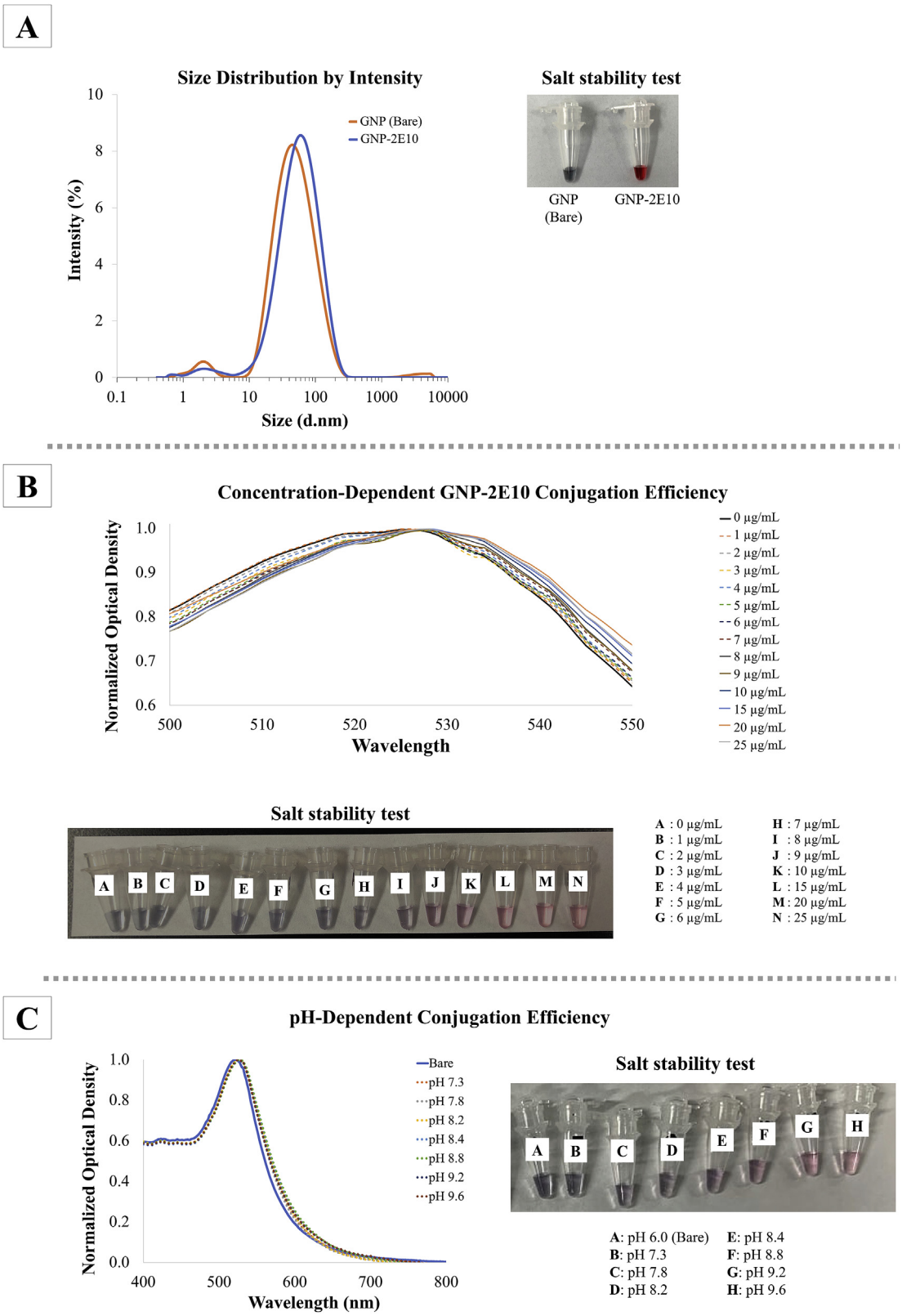

Figure 5. Characterization of GNP. (A) Hydrodynamic sizes of bare Au-GNP and antibody conjugated GNP-2E10 were assessed through dynamic light scattering by using Zetasizer. Inset shows the stable GNP-2E10 that has been optimized with suitable antibody concentration and pH of dispersion medium. The developed GNP-2E10 remained stable in 10 % (w/v) NaOH solution. Prior to upscaled production of Au-GNP-2E10, optimal (B) antibody concentration and (C) pH of dispersion medium essential for production stable conjugate were evaluated via UV-visible spectrophotometry and salt aggregation assay respectively.

The visually visible control lines on LFIA strips denote successful capillary flow of LFIA.

In oxLDL/β2GPI LFIA, oxLDL/β2GPI (antigen) formed antigen-antibody complex with biotin labelled anti-β2GPI IgG (biotin-3H3) and GNP labelled anti-apoB100 IgG (GNP-2E10). When passing the sample (containing oxLDL/β2GPI) through LFIA detection strip in the direction of the capillary flow, avidin coated on the test line of LFIA captures biotin portion of the antibody antigen complex while the conjugated GNP- 2E10 on the antibody-antigen complex provided visual qualitative assessment of oxLDL/β2GPI, presenting a purplish-red colour on both test line and control line. The intensities of the lines were measurable via ImageJ software for data analysis. Data were represented in the form of intensity of test line in relative to the intensity of its respective control line on the LFIA detection strip. Semi-quantitation of oxLDL/β2GPI was determined through a constructed four-parameter logistic curve with respect to calculated relative intensity units of known concentrations of reference standards (Cu^{2+}-oxLDL/β2GPI).

3.5. Optimization and assessment of oxLDL/β2GPI LFIA

Two different combinations of antibody conjugates for oxLDL/β2GPI LFIA systems were attempted to evaluate their respective detection efficiency and effectiveness. The two antibody conjugate combinations were: (i) Combination 1: biotin-3H3 antibody and GNP-2E10 antibody; (ii) Combination 2: biotin-2E10 antibody and GNP-3H3 antibody. Different concentrations of Cu^{2+}-oxLDL/β2GPI complexes were used as test samples. The images of developed LFIA detection strips of both systems were depicted in Figure 6A. Based upon the established standard curves (Figure 7A), antibody conjugate combination 1 acquired a better signal-to-response than antibody conjugate combination 1. From the structural perspective, oxLDL has only a copy of apoB protein (apoB100) [39,40] thus offering just an epitope recognizable by anti-apoB100 antibody (2E10 antibody) per molecule of oxLDL/β2GPI. Considering that multiple β2GPI proteins form complexes with oxLDL through specific ligand, oxLig-1, in oxLDL [18], the availability of multiple epitopes (β2GPI) recognizable by biotin-3H3 antibodies offered better contact point per molecule of oxLDL/β2GPI complex between biotin and avidin coated on the sample test line as the antibody-antigen conjugate flow across the lateral flow test strip in the direction of capillarity.

In addition, β2GPI, nLDL and oxLDL were used as negative controls to evaluate the specificity of oxLDL/β2GPI LFIA. The absences of signal on sample test line of oxLDL/β2GPI LFIA tested with β2GPI, nLDL and oxLDL (Figure 6B) denoted negative tests and unaffected interference from nLDL, oxLDL and β2GPI. The absence of non-specific binding from these tested negative controls suggested the specificity of oxLDL/β2GPI LFIA is predisposed to detection of oxLDL/β2GPI only. The detection range and sensitivity oxLDL/β2GPI LFIA and oxLDL/β2GPI ELISA were also assessed in this study. Different concentrations of Cu^{2+}-oxLDL/β2GPI complexes were applied as test samples to both detection systems. By comparing the 4PL curves derived from both detection systems for oxLDL/β2GPI (Figure 7B), it was postulated that the oxLDL/β2GPI LFIA offered a wider range of detection as compared to oxLDL/β2GPI ELISA. The 4PL standard curve oxLDL/β2GPI ELISA recorded a plateau pattern at a concentration of Cu^{2+}-oxLDL/β2GPI near 2 μg/mL. Contrarily, the oxLDL/β2GPI LFIA was capable of detecting Cu^{2+}-oxLDL/β2GPI complexes up to 50 μg/mL. In addition, respective normalized concentration-

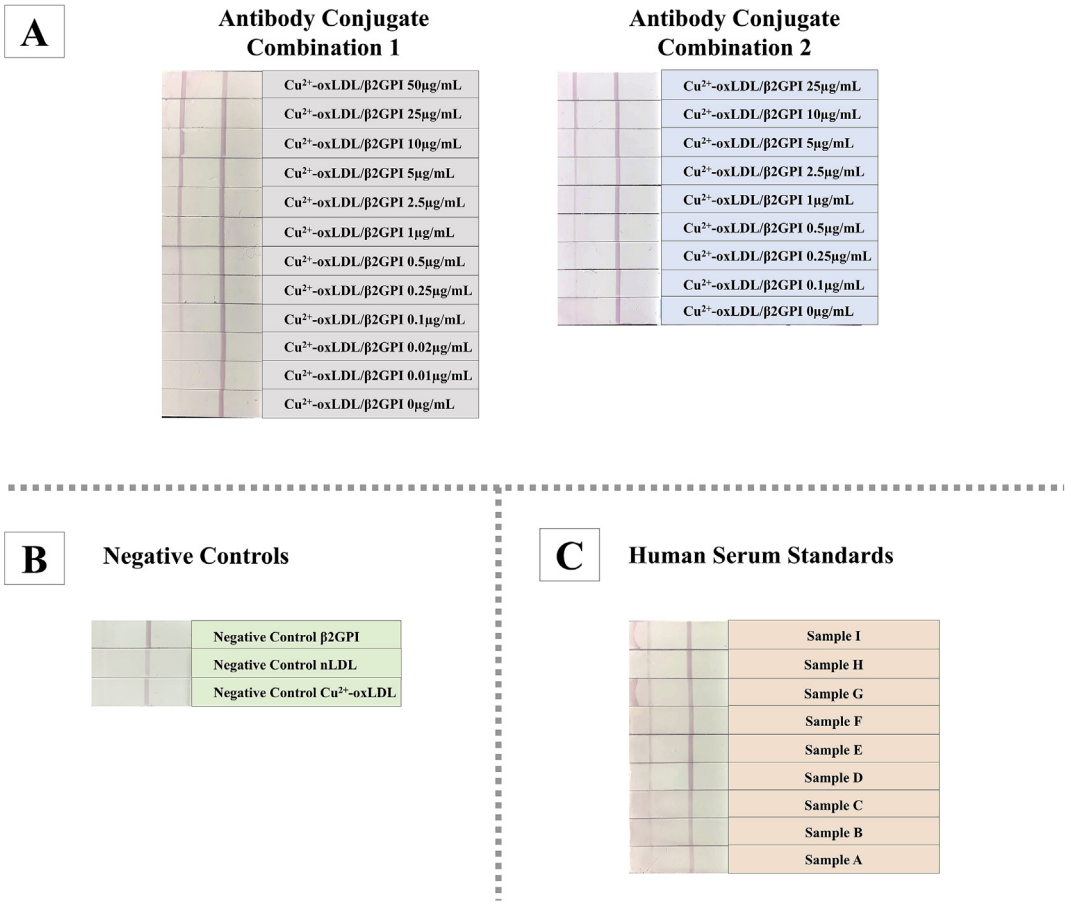

Figure 6. Respective images of developed LFIA test strips of (A) reference standards, (B) negative controls and (C) serum test samples. β2GPI, LDL and Cu^{2+}-oxLDL were tested as negative controls to evaluate specificity of oxLDL/β2GPI LFIA. Antibody conjugate combination 1 consisted of biotin-3H3 antibody + GNP-2E10 antibody while antibody conjugate combination 2 consisted of biotin-2E10 antibody + GNP-3H3 antibody.

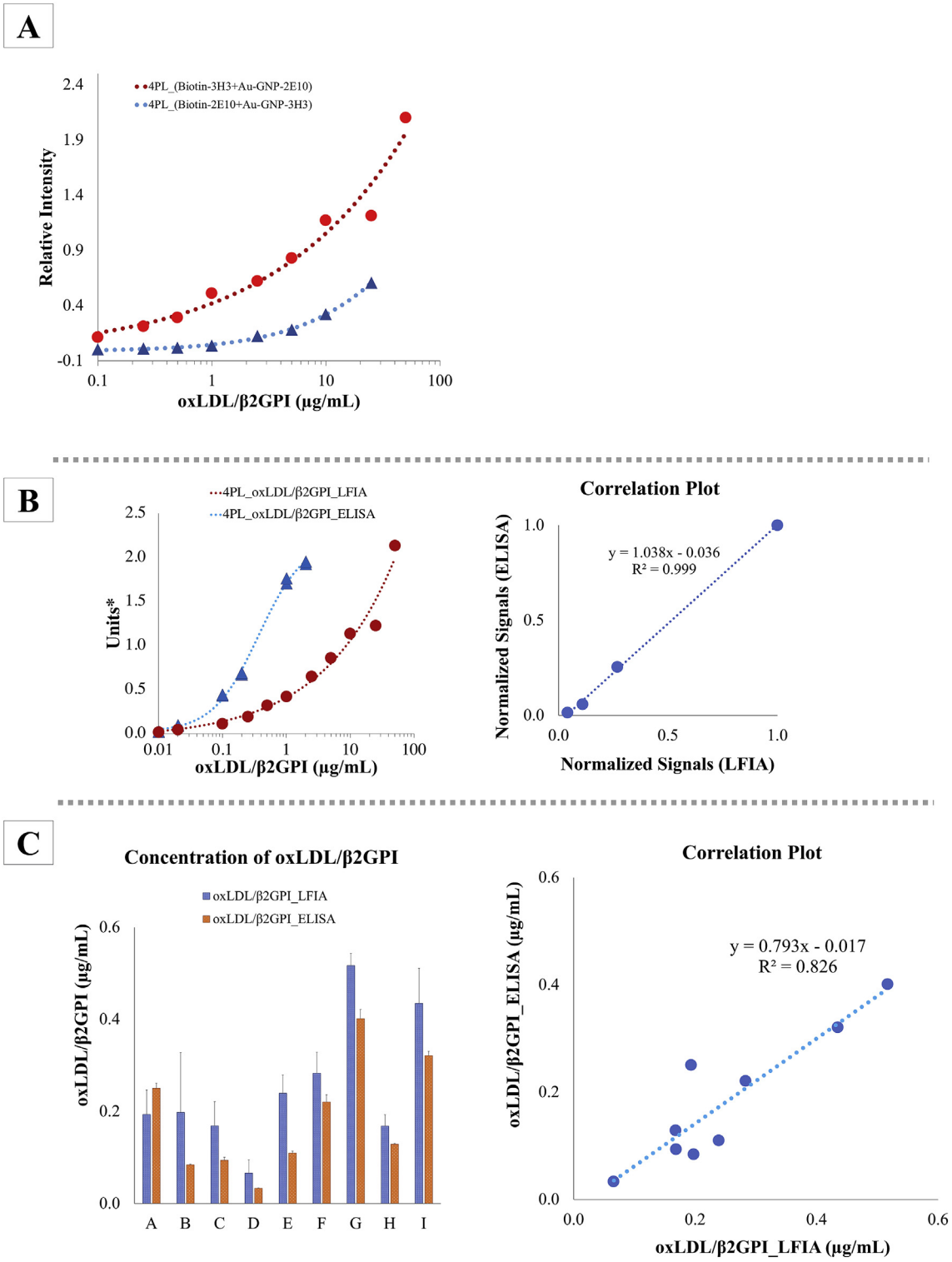

Figure 7. (A) Comparisons of four parametric logistic (4PL) curves derived from LFIA of two different antibody conjugate combinations: (1) biotin-3H3 antibody + GNP-2E10 antibody and (2) biotin-2E10 antibody + GNP-3H3 antibody. Respective images of developed LFIA test strips were depicted in Figure 6A (B) Detection sensitivity and specificity of oxLDL/β2GPI LFIA and oxLDL/β2GPI ELISA were compared by using Cu^{2+}-oxLDL/β2GPI as test sample. *Units (y-axis) for ELISA-based system were plotted in accordance to absorbance recorded at 450 nm (reference wavelength at 600 nm) while units (y-axis) for LFIA-based system were arbitrary units of relative intensities derived from ImageJ analysis. (C) OxLDL/β2GPI contents in serum samples were evaluated with oxLDL/β2GPI ELISA- and LFIA-based assay. The correlation plot showed significant correlation (R^2 value >0.826) between ELISA- and LFIA-based assay. Respective images of developed LFIA test strips were depicted in Figure 6C.

dependent signals acquired from both ELISA- and LFIA-based detection systems showed significant correlation at a R^2 value of 0.999. In terms of sensitivity, oxLDL/β2GPI LFIA was able to achieve relatively similar detection sensitivity as oxLDL/β2GPI ELISA but with an added advantage of offering a wider detection range.

3.6. Application of oxLDL/β2GPI LFIA and oxLDL/β2GPI ELISA for quantitation of oxLDL/β2GPI in unknown samples

In the present study, a total of 9 different human serum standards acquired from normal and APS/SLE patients (tested with positive anti-β2GPI IgG and oxLDL/β2GPI subgroup) were used to attest the preliminary applicability of oxLDL/β2GPI LFIA for quantitation of oxLDL/β2GPI in unknown samples. The oxLDL/β2GPI ELISA was used concurrently with similar test samples for comparisons. Different concentrations of Cu^{2+}-oxLDL/β2GPI were used as reference standard for quantitation. The quantified oxLDL/β2GPI complexes in unknown serum samples derived from both immunoassays were depicted Figure 7C. The quantified oxLDL/β2GPI through LFIA- and ELISA-based immunoassays showed significant correlation at R^2 value = 0.826 (Figure 7C).

In order to further testify the specificity of oxLDL/β2GPI LFIA, ELISA-based bioassays were employed to assess autoantibodies species present in tested serum samples by using oxLDL and β2GPI as antigens for anti-oxLDL and anti-β2GPI autoantibodies. Correlation plot of O.D acquired from each ELISA assay was plotted against the concentration of oxLDL/β2GPI detected in serum samples by means of ELISA and LFIA (Figures 8A-8C). It was demonstrated in this study that the anti-β2GPI IgG titers in tested serum samples were significantly correlated with the presence of of oxLDL/β2GPI (R^2 value >0.5) (Figure 8A). It has been established that APS/SLE patients attain high serological titre of auto-anti-β2GPI IgG and develop clinical features of atherosclerotic complications [41]. β2GPI acts as a major antigen for antiphospholipid autoantibodies in APS patients when it binds to anionic phospholipids and the resulting immunogenic complex is thought to augment the advancement of atherogenic complications of APS [9, 10, 11, 12]. The proatherogenic effects of such immune complexes were further evidently asserted when oxLDL/β2GPI, with anti-β2GPI IgG alongside, were internalized more rapidly by macrophages through their Fcγ receptors [14].

There was significant correlation (R^2 value >0.16) between anti-oxLDL IgG and concentration of oxLDL/β2GPI (Figure 8B) which suggested the prevalence of autoantibodies against oxLDL in tested serum samples. High serological titer of oxLDL is a common prognosis of autoimmune disease patients and patients with atherosclerotic complications. OxLDL is perceived as an immunogen held accountable for induction of anti-oxLDL autoantibodies. A positive correlation between

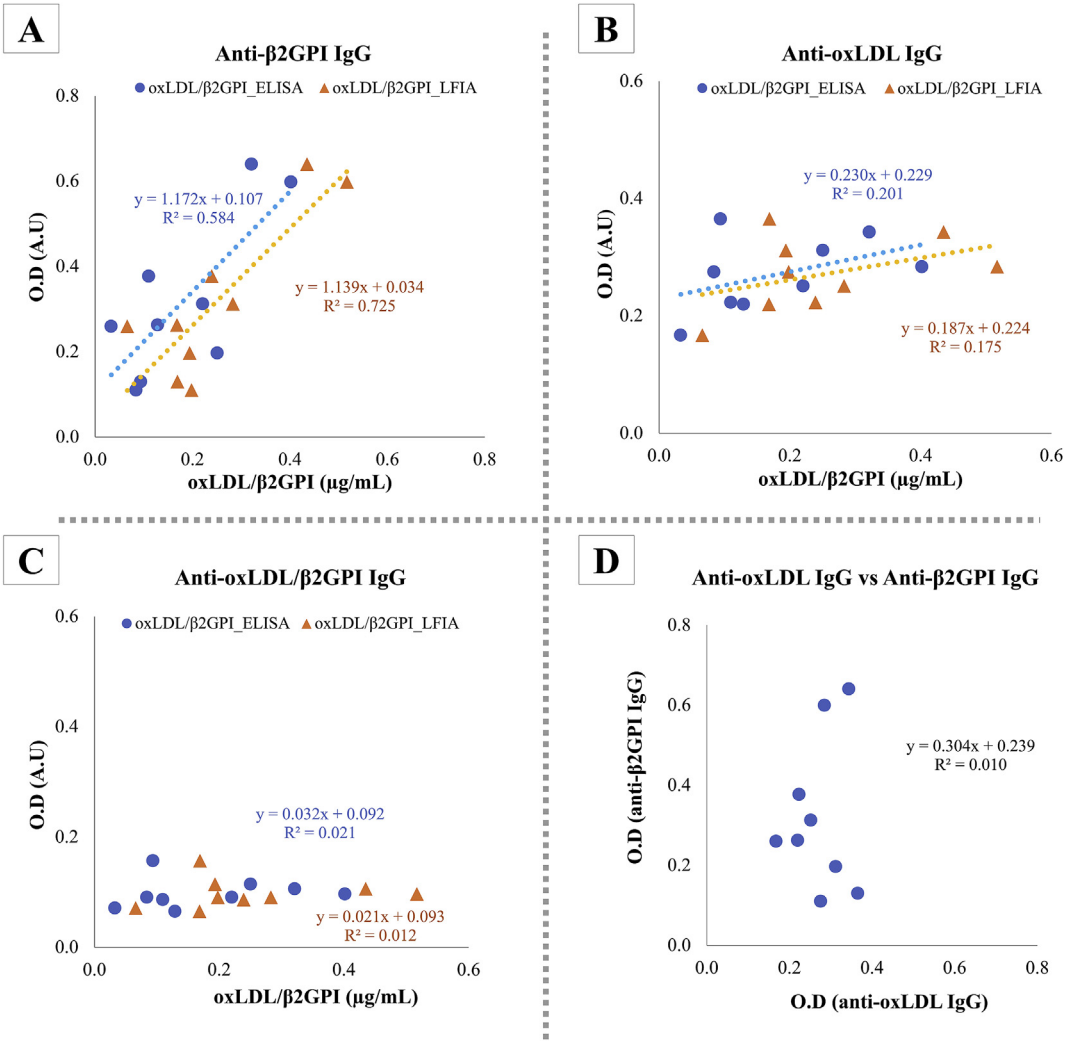

Figure 8. The presences of anti-β2GPI, anti-oxLDL, and anti-oxLDL/β2GPI IgG in serum samples were tested via solid-phase ELISA. Correlativity of respective antibodies: (A) anti-β2GPI IgG; (B) anti-oxLDL IgG; (C) anti-oxLDL/β2GPI IgG was plotted against concentration of oxLDL/β2GPI in serum samples as tested with oxLDL/β2GPI ELISA and LFIA. Correlation curve anti-β2GPI IgG versus anti-oxLDL IgG (D) was plotted accordingly to evaluate the inter-relativity.

serological titers of anti-oxLDL antibodies and severity of atherosclerosis related complications was established previously [42, 43, 44, 45].

However, there was no correlation between concentration of oxLDL/β2GPI and anti-oxLDL/β2GPI IgG (R^2 = 0.01–0.02) (Figure 8C). As chemically synthesized oxLDL/β2GPI was coated as antigen on ELISA plate to measure anti-oxLDL/β2GPI IgG titer from tested serum samples, it was postulated that the density of β2GPI portion of oxLDL/β2GPI coated on ELISA plate as epitope detectable by anti-oxLDL/β2GPI IgG in tested serum titers remained limited. The apolipoprotein B-containing oxLDL is a relatively huge lipid vesicle as compared to β2GPI. Contrary to the direct coating of β2GPI only as solid phase antigen for ELISA, it is postulated that the sheer size of oxLDL portion of the oxLDL/β2GPI complex may have incurred stearic hindrance which lowers the absolute effective coating density of Cu^{2+}-oxLDL/β2GPI on the surface of ELISA. The resulting steric hindrance may have caused epitope-masking, and hence resulted in underestimation of anti-oxLDL/β2GPI IgG. Nonetheless, the prevalence of these autoantibodies in tested serum titers did not affect the specificity of oxLDL/β2GPI LFIA.

Lipid and lipoprotein metabolic abnormalities are closely associated with hyperlipidemia and high levels of plasma LDL and oxLDL. These are factored as part of the fundamental contributing factors leading to the onset and progression of atherosclerotic cardiovascular complication and mortality [46, 47]. The discovery of atherogenic oxLDL/β2GPI complexes in sera of APS patients has been considered as one of the quantifiable risk factors for clinical manifestation of arterial thrombosis in APS [41]. However, such atherogenic complexes were also discovered in patients of non-systemic autoimmune diseases, such as diabetes mellitus [24] and chronic nephritis [25]. These sightings may warrant attention concerning the clinical implications of these circulating oxLDL/β2GPI complexes as potential diagnostic biomarker for risk stratification of atherosclerotic complications.

Although serological levels of oxLDL/β2GPI complexes are assessible by means of ELISA, its sustainability and high-throughput productivity are discredited by the common shortfalls of ELISA for being complicated, time- and cost-inefficient. Current preliminary outcomes suggested comparative specificity between LFIA- and ELISA-based oxLDL/β2GPI assays, hence offering a theoretical insight for future feasible clinical applicability of oxLDL/β2GPI LFIA as a mean of high-throughput diagnostic and risk stratification tool for atherosclerosis-related complications. However, it is worth to note that more serum samples are to be tested further with oxLDL/β2GPI LFIA to fully ascertain its future applicability for in clinical settings. By testing the oxLDL/β2GPI in serum samples of a large cohort comprising of different study populations (normal controls, mild and severe disease population), the lower and upper precision limits of the oxLDL/β2GPI LFIA can be determined to prevent underestimation or overestimation of detection outputs. These validations remain necessary to further complement the diagnostic sensitivity and specificity of present oxLDL/β2GPI LFIA prototype for future feasible clinical application. Nonetheless, oxLDL/β2GPI LFIA remains advantageous over the oxLDL/β2GPI ELISA. The unrequired washing step and relatively short developmental and analysis time allow a high throughput screening as opposed to the laborious and tedious conventional ELISA system. In addition, the system offers high levels of customizations and requires low technical comprehensiveness. Due to its simplicity, applications at point of care or need can be easily performed by individuals accordingly.

4. Conclusion

The developed oxLDL/β2GPI LFIA offers a simple test procedure to quantitatively assess oxLDL/β2GPI in serum or sample containing the same. The sensitivity and precision of oxLDL/β2GPI LFIA were comparable to oxLDL/β2GPI ELISA. The approach requires low technical comprehensiveness and requires only small sample volumes. The unrequired sample pre-treatment and washing steps support fast analysis as it requires a relatively short 20 min developmental time, as opposed to 3 h required by the application of ELISA. Owing to its simplificity, oxLDL/β2GPI LFIA supports potential point-of-care application in future, particularly for high-throughput diagnosis and risk stratification of atherosclerosis-related complications.

Declarations

Author Contribution statement

X. Tan: Conceived and designed the experiments; Performed the experiments; Analyzed and interpreted the data; Contributed reagents, materials, analysis tools or data; Wrote the paper.

F. Takenaka: Conceived and designed the experiments; Contributed reagents, materials, analysis tools or data.

H. Takekawa: Performed the experiments.

E. Matsuura: Conceived and designed the experiments; Analyzed and interpreted the data; Contributed reagents, materials, analysis tools or data; Wrote the paper.

Funding statement

E. Matsuura was supported by Ministry of Education, Culture, Sports, Science and Technology.

Competing interest statement

The authors declare no conflict of interest.

Additional information

No additional information is available for this paper.

References

[1] A.D. Mooradian, Dyslipidemia in type 2 diabetes mellitus, Nat. Clin. Pract. Endocrinol. Metab. 5 (2009) 150–159.
[2] W. Palinski, M.E. Rosenfeld, S. Ylä-Herttuala, G.C. Gurtner, S.S. Socher, S.W. Butler, S. Parthasarathy, T.E. Carew, D. Steinberg, J.L. Witztum, Low density lipoprotein undergoes oxidative modification *in vivo*, Proc. Natl. Acad. Sci. U. S. A 86 (4) (1989) 1372–1376.
[3] P. Libby, Inflammation in atherosclerosis, Nature 420 (6917) (2002) 868–874.
[4] G.K. Hansson, Inflammation, atherosclerosis, and coronary artery disease, N. Engl. J. Med. 352 (16) (2005) 1685–1695.
[5] K. Ichikawa, M.A. Khamashta, T. Koike, E. Matsuura, G.R.V. Hughes, β2-glycoprotein I reactivity of monoclonal anticardiolipin antibodies from patients with the antiphospholipid syndrome, Arthritis Rheum. 37 (10) (1994) 1453–1461.
[6] M.L. Boey, C.B. Colaco, A.E. Gharavi, K.B. Elkon, S. Loizou, G.R.V. Hughes, Thrombosis in systemic lupus erythematosus: striking association with the presence of circulating lupus anticoagulant, Br. Med. J. (Clin Res Ed) 287 (6398) (1983) 1021–1023.
[7] G.R.V. Hughes, N.N. Harris, A.E. Gharavi, The anticardiolipin syndrome, J. Rheumatol. 13 (3) (1986) 486–489.
[8] E.N. Harris, M.L. Boey, C.G. Mackworth-Young, A.E. Gharavi, B.M. Patel, S. Loizou, G.R.V. Hughes, Anticardiolipin antibodies: detection by radioimmunoassay and association with thrombosis in systemic lupus erythematosus, Lancet 322 (8361) (1983) 1211–1214.
[9] E. Matsuura, Y. Igarashi, M. Fujimoto, K. Ichikawa, T. Koike, Anticardiolipin cofactor(s) and differential diagnosis of autoimmune disease, Lancet 336 (8708) (1990) 177–178.
[10] E. Matsuura, Y. Igarashi, M. Fujimoto, K. Ichikawa, T. Suzuki, T. Sumida, T. Yasuda, T. Koike, Heterogeneity of anticardiolipin antibodies defined by the anticardiolipin cofactor, J. Immunol. 148 (12) (1992) 3885–3891.
[11] H.P. McNeil, R.J. Simpson, C.N. Chesterman, S.A. Krilis, Anti-phospholipid antibodies are directed against a complex antigen that includes a lipid-binding inhibitor of coagulation: β2-glycoprotein I (apolipoprotein H), Proc. Natl. Acad. Sci. U.S.A. 87 (11) (1990) 4120–4124.
[12] M. Galli, P. Comfurius, C. Maassen, H.C. Hemker, M.H. de Baets, P.J. van Breda-Vriesman, T. Barbui, R.F. Zwaal, E.M. Bevers, Anticardiolipin antibodies (ACA) directed not to cardiolipin but to a plasma protein cofactor, Lancet 335 (8705) (1990) 1544–1547.
[13] N.S. Lee, H.B. Brewer, J.C. Osborne, β2-glycoprotein I. Molecular properties of an unusual apolipoprotein, apolipoprotein H, J. Bio. Chem. 258 (8) (1983) 4765–4770.
[14] Y. Hasunuma, E. Matsuura, Z. Makita, T. Katahira, S. Nishi, T. Koike, Involvement of β2-glycoprotein I and anticardiolipin antibodies in oxidatively modified low-density lipoprotein uptake by macrophages, Clin. Exp. Immunol. 107 (3) (1997) 569–573.

[15] J.E. Hunt, R.J. Simpson, S.A. Krilis, Identification of a region of β2-glycoprotein I critical for lipid binding and anti-cardiolipin antibody cofactor activity, Proc. Natl. Acad. Sci. U.S.A. 90 (6) (1993) 2141–2145.
[16] H. Kato, K. Enjyoji, Amino acid sequence and location of the disulfide bonds in bovine β2-glycoprotein I: the presence of five Sushi domains, Biochemistry 30 (50) (1991) 11687–11694.
[17] J.E. Hunt, S.A. Krilis, The fifth domain of β2-glycoprotein I contains a phospholipid binding site (Cys281-Cys288) and a region recognized by anticardiolipin antibodies, J. Immunol. 152 (2) (1994) 653–659.
[18] K. Kobayashi, E. Matsuura, Q. Liu, J.-i. Furukawa, K. Kaihara, J. Inagaki, T. Atsumi, N. Sakairi, T. Yasuda, D.R. Voelker, T. Koike, A specific ligand for β2-glycoprotein I mediates autoantibody-dependent uptake of oxidized low density lipoprotein by macrophages, J. Lipid Res. 42 (5) (2001) 697–709.
[19] E. Matsuura, K. Kobayashi, M. Tabuchi, L.R. Lopez, Oxidative modification of low-density lipoprotein and immune regulation of atherosclerosis, Prog. Lipid Res. 45 (6) (2006) 466–486.
[20] K. Kobayashi, K. Tada, H. Itabe, T. Ueno, P.H. Liu, A. Tsutsumi, M. Kuwana, T. Yasuda, Y. Shoenfeld, P.G. de Groot, E. Matsuura, Distinguished effects of antiphospholipid antibodies and anti-oxidized LDL antibodies on oxidized LDL uptake by macrophages, Lupus 16 (12) (2007) 929–938.
[21] T. Kajiwara, T. Yasuda, E. Matsuura, Intracellular trafficking of β2-glycoprotein I complexes with lipid vesicles in macrophages: implications on the development of antiphospholipid syndrome, J. Autoimmun. 29 (2) (2007) 164–173.
[22] Y. Yamaguchi, N. Seta, J. Kaburaki, K. Kobayashi, E. Matsuura, M. Kuwana, Excessive exposure to anionic surfaces maintains autoantibody response to β2-glycoprotein I in patients with antiphospholipid syndrome, Blood 110 (13) (2007) 4312–4318.
[23] D. Lopez, I. Garcia-Valladares, C.A. Palafox-Sanchez, I.G. De La Torre, K. Kobayashi, E. Matsuura, L.R. Lopez, Oxidized low-density lipoprotein/β2-glycoprotein I complexes and autoantibodies to oxLig-1/β2-glycoprotein I in patients with systemic lupus erythematosus and antiphospholipid syndrome, Am. J. Clin. Pathol. 121 (3) (2004) 426–436.
[24] L.R. Lopez, B.L. Hurley, D.F. Simpson, E. Matsuura, Oxidized low-density lipoprotein/β2-glycoprotein I complexes and autoantibodies in patients with type 2 diabetes mellitus, Ann. N. Y. Acad. Sci. 1051 (1) (2005) 97–103.
[25] J. Kasahara, K. Kobayashi, Y. Maeshima, Y. Yamasaki, T. Yasuda, E. Matsuura, H. Makino, Clinical significance of serum oxidized low-density lipoprotein/β2-glycoprotein I complexes in patients with chronic renal diseases, Nephron. Clin. Practi. 98 (1) (2004) c15–c24.
[26] Ç. Ağar, G.M.A. van Os, M. Mörgelin, R.R. Sprenger, J.A. Marquart, R.T. Urbanus, R.H.W.M. Derksen, J.C.M. Meijers, P.G. de Groot, β2-glycoprotein I can exist in 2 conformations: implications for our understanding of the antiphospholipid syndrome, Blood 116 (8) (2010) 1336–1343.
[27] F.H. Passam, B. Giannakopoulos, P. Mirarabshahi, S.A. Krilis, Molecular pathophysiology of the antiphospholipid syndrome: the role of oxidative post-translational modification of beta 2 glycoprotein I, J. Thromb. Haemostasis 9 (s1) (2011) 275–282.
[28] T. Sasaki, K. Kobayashi, S. Kita, K. Kojima, H. Hirano, L. Shen, F. Takenaka, H. Kumon, E. Matsuura, In vivo distribution of single chain variable fragment (scFv) against atherothrombotic oxidized LDL/β2-glycoprotein I complexes into atherosclerotic plaques of WHHL rabbits: implication for clinical PET imaging, Autoimmun. Rev. 16 (2) (2017) 159–167.
[29] P.R. Ames, A. Ortiz-Cadenas, I.G.-D.L. Torre, A. Nava, A. Oregon-Miranda, J.R. Batuca, K. Kojima, L.R. Lopez, E. Matsuura, Rosuvastatin treatment is associated with a decrease of serum oxidised low-density lipoprotein/β2-glycoprotein I complex concentration in type 2 diabetes, Br. J. Diabetes Vasc. Dis. 10 (6) (2010) 292–299.
[30] K.M. Koczula, A. Gallotta, Lateral flow assays, Essays Biochem. 60 (1) (2016) 111–120.
[31] C.S. Kosack, A.L. Page, P.R. Klatser, A guide to aid the selection of diagnostic tests, in: W.H.O.(WHO (Ed.), Bulletin of the World Health Organization, World Health Organization (WHO), 2017.
[32] D.W. Swinkels, H.L. Hak-Lemmers, P.N. Demacker, Single spin density gradient ultracentrifugation method for the detection and isolation of light and heavy low density lipoprotein subfractions, J. Lipid Res. 28 (10) (1987) 1233–1239.
[33] H. Ohkawa, N. Ohishi, K. Yagi, Assay for lipid peroxides in animal tissues by thiobarbituric acid reaction, Anal. Biochem. 95 (2) (1979) 351–358.
[34] P. Chun, Colloidal gold and other labels for lateral flow immunoassays, in: R. Wong, H. Tse (Eds.), Lateral Flow Immunoassay, Humana Press, Totowa, NJ, 2009, pp. 1–19.
[35] X. Huang, M.A. El-Sayed, Gold nanoparticles: optical properties and implementations in cancer diagnosis and photothermal therapy, J. Adv. Res. 1 (1) (2010) 13–28.
[36] S. Dominguez-Medina, J. Blankenburg, J. Olson, C.F. Landes, S. Link, Adsorption of a protein monolayer via hydrophobic interactions prevents nanoparticle aggregation under harsh environmental conditions, ACS Sustain. Chem. Eng. 1 (7) (2013) 833–842.
[37] E.L.L. Yeo, A.J.S. Chua, K. Parthasarathy, H.Y. Yeo, M.L. Ng, J.C.Y. Kah, Understanding aggregation-based assays: nature of protein corona and number of epitopes on antigen matters, RSC Adv. 5 (20) (2015) 14982–14993.
[38] G. Ruiz, K. Tripathi, S. Okyem, J.D. Driskell, pH impacts the orientation of antibody adsorbed onto gold nanoparticles, Bioconjugate Chem. 30 (4) (2019) 1182–1191.
[39] J.P. Segrest, M.K. Jones, H. De Loof, N. Dashti, Structure of apolipoprotein B-100 in low density lipoproteins, J. Lipid Res. 42 (9) (2001) 1346–1367.
[40] S.-y. Morita, Metabolism and modification of apolipoprotein b-containing lipoproteins involved in dyslipidemia and atherosclerosis, Biol. Pharm. Bull. 39 (1) (2016) 1–24.
[41] K. Kobayashi, M. Kishi, T. Atsumi, M.L. Bertolaccini, H. Makino, N. Sakairi, I. Yamamoto, T. Yasuda, M.A. Khamashta, G.R.V. Hughes, T. Koike, D.R. Voelker, E. Matsuura, Circulating oxidized LDL forms complexes with β2-glycoprotein I: implication as an atherogenic autoantigen, J. Lipid Res. 44 (4) (2003) 716–726.
[42] J.T. Salonen, H. Korpela, R. Salonen, K. Nyyssonen, S. Yla-Herttuala, R. Yamamoto, S. Butler, W. Palinski, J.L. Witztum, Autoantibody against oxidised LDL and progression of carotid atherosclerosis, Lancet 339 (8798) (1992) 883–887.
[43] G. Virella, I. Virella, R.B. Leman, M.B. Pryor, M.F. Lopes-Virella, Anti-oxidized low-density lipoprotein antibodies in patients with coronary heart disease and normal healthy volunteers, Int. J. Clin. Lab. Res. 23 (1) (1993) 95–101.
[44] J.T. Cvetkovic, S. Wållberg-Jonsson, E. Ahmed, S. Rantapää-Dahlqvist, A.K. Lefvert, Increased levels of autoantibodies against copper-oxidized low density lipoprotein, malondialdehyde-modified low density lipoprotein and cardiolipin in patients with rheumatoid arthritis, Rheumatology 41 (9) (2002) 988–995.
[45] Y. Shoenfeld, R. Wu, D. Dearing Linda, E. Matsuura, Are anti–oxidized low-density lipoprotein antibodies pathogenic or protective? Circulation 110 (17) (2004) 2552–2558.
[46] J.W. Heinecke, Mechanisms of oxidative damage of low density lipoprotein in human atherosclerosis, Curr. Opin. Lipidol. 8 (5) (1997) 268–274.
[47] D. Steinberg, Low density lipoprotein oxidation and its pathobiological significance, J. Biol. Chem. 272 (34) (1997) 20963–20966.